

S. Nam, A.E. Ashtiani, C.F. Oztek-Yerli and I.D. Robertson (Microwave Circuits and Devices Group, Department of Electronic Engineering, King's College London, Strand, London WC2R 2LS, United Kingdom)

E-mail: nam@orion.eee.kcl.ac.uk

References

- LUCYSZYN, S., and ROBERTSON, I.D.: 'Analogue reflection topology building blocks for adaptive microwave signal processing applications', *IEEE Trans. Microw. Theory Tech.*, 1995, 43, (3), pp. 601-611
- DEVLIN, L.M., and MINNIS, B.J.: 'A versatile vector modulator design for MMIC'. *IEEE MTT-S Int. Symp. Dig.*, 1990, pp. 519-522
- UPSHUL, J.I., and GELLER, B.D.: 'Low-loss 360° X-band phase shifter'. *IEEE MTT-S Int. Symp. Dig.*, 1990, pp. 487-490
- GOLDFARB, M.E., and PLATZKER, A.: 'A wide range analogue MMIC attenuator with integral 180° phase shifter', *IEEE Trans. Microw. Theory Tech.*, 1994, 42, (1), pp. 156-158
- LUCYSZYN, S., YERLI, C.F.O., and ROBERTSON, I.D.: 'Accurate modelling of cold-MESFETs for adaptive signal processing applications'. 25th EuMc, Bologna, September 1995

Double correlating interferometer scheme for measuring PM and AM noise

E. Rubiola, V. Giordano and J. Gros Lambert

A new scheme is proposed to measure close-to-carrier PM and AM noise by means of correlation between two interferometric measurements. The most relevant feature is the ability to reject interferometric system noise, thus improving the sensitivity. Implementation and experimental results are discussed.

Introduction: An interferometric method for measuring close-to-carrier phase and amplitude noise of a microwave device is an old idea [1] that has recently revived the interest of the frequency metrology community after some impressive results, such as [2], published by the University of Western Australia.

The principle of the interferometric system is shown in Fig. 1. The phase shift γ and the attenuation l are set equal to those of the device under test (DUT). The hybrid coupler makes the sum and the difference, i.e. the interference, of its input signals. Hence, all the carrier power goes to the Σ output of the hybrid, while at Δ output only the DUT noise sidebands are present. Letting $s(t) = \sqrt{2c}[1 + \epsilon(t)]\cos[2\pi f_c t + \phi(t)]$ for the DUT output signal, the FFT analyser measures $S_{\phi}(f)$ or $S_{\epsilon}(f)$, i.e. the power spectrum density (PSD) of PM or AM noise, depending on the detection phase γ' . Results are reported using $L(f) = S_{\phi}(f)/2$ and expressed in dBc/Hz; $L(f)$ and dBc/Hz are also used for AM noise.

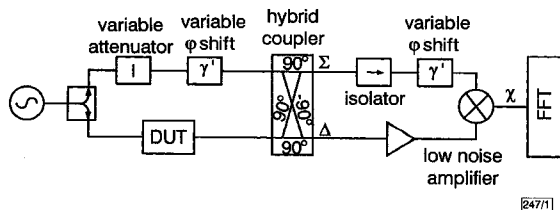


Fig. 1 Interferometric PM and AM noise measurement system

Nonlinearity is responsible of the amplifiers close-to-carrier noise, which is generated by upconverting the DC bias noise [3]. Consequently, carrier suppression is needed to keep the amplifier in its fully linear region, thus keeping the amplifier noise at its minimum. Hence, the theoretical noise floor of the described system comes from the interferometer equivalent temperature and the amplifier noise figure. Since $kT = -174\text{dBm/Hz}$ at room temperature, a noise floor $L(f) = -185\text{dBc/Hz}$ would be expected in a

system in which the amplifier noise figure is $F = 2\text{dB}$ and the carrier power is 10dBm . A noise floor some decibels higher than that can be practically attained. Moreover, flicker noise of the interferometer components, mainly the variable attenuator and phase shifter, further limits the system sensitivity. This last limitation makes it difficult to automatically tune the carrier suppression because electrically controlled attenuators and shifters are generally more noisy than the manually adjustable ones.

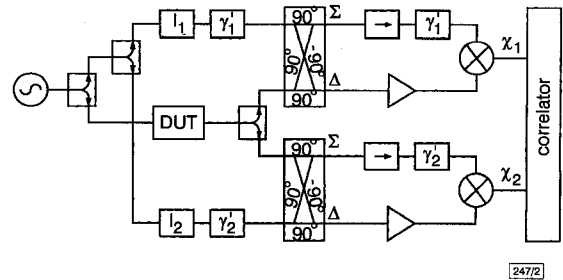


Fig. 2 Double correlating interferometer scheme

Double correlating interferometer: The new scheme that we propose (Fig. 2) involves building two equal interferometric systems around one DUT and correlating their outputs. Letting K be the interferometer's power gain, N_D , N_1 and N_2 the noise PSD of the DUT and the two interferometers, respectively, the PSDs at the mixers output (which is the noise down converted to baseband) are $S_{x_1}(f) = K(N_D + N_1)$ and $S_{x_2}(f) = K(N_D + N_2)$. Since N_1 and N_2 originate in different devices, they are uncorrelated and, consequently, the cross PSD $S_{x_1x_2}(f)$ turns out to be equal to KN_D . This mechanism allows measuring the DUT noise and rejecting the interferometers noise. At a closer sight, the noise reduction capability of the correlation mechanism turns out to be limited by the isolation between the two interferometers and by the power splitters noise, which gives partially correlated contributions to x_1 and x_2 . Nevertheless, a noise reduction of up to 30dB seems to be feasible, depending on the implementation and the operating conditions.

We implemented our scheme to operate at the frequency $f_c = 7.3\text{GHz}$, chosen because of the availability of all the components. Our primary interest is the noise of the system itself and consequently we measured a null DUT, i.e. a short cable.

In our prototype the DUT power is 15dBm ; the amplifiers show a gain $g_a = 43\text{dB}$, a bandwidth of 250MHz and a maximum output power $P_m = 18\text{dBm}$. After a careful tuning, a carrier suppression of -80 to -90dB can be achieved, stable for a few tens of minutes. In this condition the carrier is at least 40dB lower than P_m , thus ensuring the amplifiers linearity.

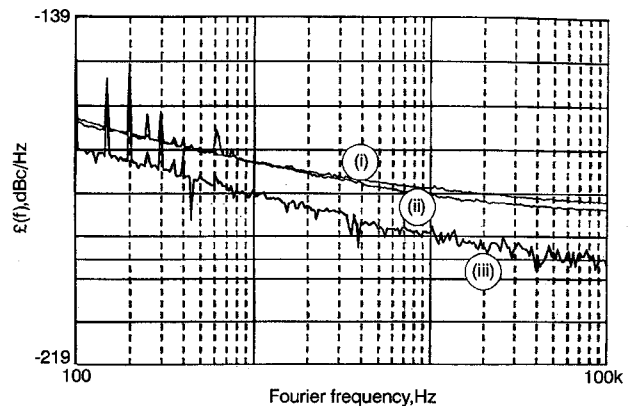


Fig. 3 Instrumental noise of double correlating interferometer

(i), (ii) noise at the two interferometers' outputs; (iii) cross spectrum noise, i.e. system sensitivity

Experimental results: In our prototype, the isolation between the two interferometers, measured by injecting a sideband in one interferometer and observing the output of the other one, is close to 60dB. This isolation value limits the noise rejection by correlation to 30dB. Detection phases γ'_1 and γ'_2 were set equal by injecting a

suitable modulation in the DUT signal path through a directional coupler and nulling the output signals. Similarly, the system gain K was measured as the ratio between the output signal and an injected modulation.

As the source noise rejection turned out to be 70–80 dB and the noise of microwave oscillators is high as compared to the expected noise of our system, we used the best available source. Thus, the system was driven by a cryogenic whispering gallery sapphire oscillator which exhibits a white noise of -183 dBc/Hz and an estimated flicker noise of -97 dBc/Hz at 100 Hz. The results, measured with the cryogenic oscillator and the null DUT, are shown in Fig. 3. Curves (i) and (ii) of this Figure are $L_{x_1}(f)$ and $L_{x_2}(f)$, measured at the two mixer outputs, while curve (iii) is the cross PSD $L_{x_1x_2}(f)$, i.e. the system noise floor. In the leftmost part of the plot, for $f < 10$ kHz, the system noise is -170 dBc/Hz at 100 Hz with slope f^{-1} . The full noise rejection capability of our system, which would be due to the two arms isolation, cannot be attained in this experiment because of the source noise, which is still too high. In the rightmost part of the plot, for $f > 20$ kHz, the slope of curve (iii) approaches the white noise floor. Unfortunately, the value of the latter can only be inferred because of the insufficient frequency range of the available FFT. Anyway, the white noise floor is not higher than -195 dBc/Hz.

Conclusions: The double correlating interferometer scheme allows PM and AM noise measurements with a lower instrument noise as compared to single interferometer systems. Our microwave prototype, although not optimised, proves the feasibility and the benefits of the proposed scheme. Both HF and VHF realisation, based on commercially available parts, are also possible. Finally, noise reduction by correlation makes feasible an automatically tuned version of our scheme, bypassing the limitation due to the higher noise of the voltage controlled attenuators and shifter, as compared with those that are manually adjustable.

© IEE 1998

4 November 1997

Electronics Letters Online No: 19980129

E. Rubiola (Politecnico di Torino, Dipartimento di Elettronica, c. Duca degli Abruzzi n. 24, I-10129 Torino, Italy)

E-mail: rubiola@polito.it

V. Giordano and J. Gros Lambert (Laboratoire de Physique et Metrologie des Oscillateurs (LPMO), 32, avenue de l'Observatoire, 25000 Besancon, France)

E-mail: giordano@lpmo.univ-fcomte.fr

Corresponding author: E. Rubiola

References

- 1 SANN, K.H.: 'The measurement of near-carrier noise in microwave amplifiers', *IEEE Trans. Microw. Theory Tech.*, 1968, **MTT-16**, (9), pp. 761–766
- 2 IVANOV, E.N., TOBAR, M.E., and WOODE, R.A.: 'A study of noise phenomena in microwave components using an advanced noise measurement system', *IEEE Trans. Ultrason. Ferroelectr. Freq. Control.*, 1997, **44**, (1), pp. 161–163
- 3 WALLS, F.L., FERRE-PIKAL, E.S., and JEFFERTS, S.R.: 'Origin of $1/f$ pm and am noise in bipolar junction transistor amplifiers', *IEEE Trans. Ultrason. Ferroelectr. Freq. Control.*, 1997, **44**, (2), pp. 326–334

Dual antenna concept for simultaneous thermography and hyperthermic heating

S. Jacobsen

The sensitivity of microwave radiometry for detecting subcutaneous targets is strongly related to the antenna receiving properties. When radiometry is used in conjunction with superficial hyperthermia, there are conflicting requirements in optimising the antenna design for both tasks. The authors therefore propose an integrated tranceiving antenna approach for simultaneous heating and thermometry. By means of a scanning electric field probe, the radiated electric field distribution was measured for the concept in an homogeneous lossy medium.

Introduction: It is known that microwave radiometry (the measurement of electromagnetic radiation from matter at microwave frequencies) can be used as a gauge-principle for retrieval of thermal gradients related to pathological conditions inside the human body [1, 2]. Because of the relatively moderate absorption of microwaves in living tissue, it is acknowledged that this technique is able to provide information on the absolute tissue temperature to depths of several centimeters [3]. An important consideration in this connection is the effective depth of sensing. The sensing occurs in the extreme near field of the antenna with a sensitivity function that is strongly affected by both the antenna geometry (which implicitly influences the antenna coupling and radiation characteristics) and material properties. As a consequence, the sensing depth will be smaller than the upper theoretical limit for plane-wave propagation provided by an infinitely large aperture. Thus, the critical component limiting the system performance is the antenna [4]. The effective aperture area determines the amount of thermal energy received. Since the emission is also frequency dependent, the information carried by measurement at different frequency bands may be used to reconstruct temperature profiles in the tissue. The optimum antenna design for detection of weak noise signals is therefore a broadband directive antenna providing a centrally situated narrow main lobe. This demand must in turn be balanced against the need for transversal spatial resolution which is inversely proportional to antenna size. Presently, a one arm microstrip spiral antenna concept is investigated for its usefulness as a broadband receiver to meet these criteria.

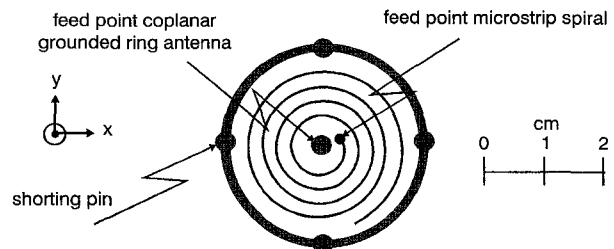


Fig. 1 Schematic representation of microstrip tranceiving antenna concept

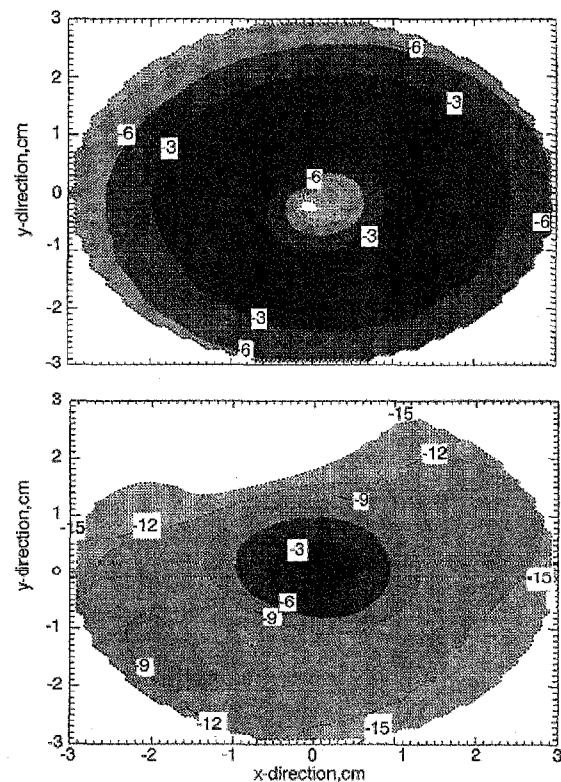


Fig. 2 Measured 2D power deposition patterns (dB scale) 1.5 cm deep in muscle phantom at 1400 MHz

- a Microstrip coplanar grounded ring antenna
b Microstrip spiral antenna